

Modelling the Effect of Incompressible Leakage Patterns on Rupture Area in Pipeline

M. Shehadeh^{1*} and A.I. Shahata²

¹ Marine Engineering Department, College of Engineering and Technology
Arab academy for science, technology and Maritime Transport, EGYPT

² Mechanical Engineering Department, College of Engineering
Arab academy for science, technology and Maritime Transport, EGYPT

Received: 07/09/2013 – Revised 29/11/2013 – Accepted 06/12/2013

Abstract

This paper presents a three-dimensional numerical analysis for rupture area in steel pipeline using a general-purpose CFD solver. A computational model is developed for studying leakage in steel pipes with different rupture diameters and different fluid flow properties such as pressures and velocity. The simulation results showed a good agreement with experimental measurements. Numerical solutions for the distributions of water flow velocity, pressure and turbulence are presented and discussed. The results show that there is a direct relation between the maximum velocity, total pressure, turbulence intensity and leakage mass flow rate with rupture area in pipelines.

Keywords: Pipeline; Leakage Water; Modelling; CFD; Rupture Area.

1. Introduction

Leak detection systems are one of the paramount concerns of pipeline operators all over the world which depend heavily on leak size [1]. Better understanding of the liquid properties and conditions can lead to improve the pipelines systems requirements. Moreover, high risk fields such as oil and gas industry can be designed with leak detection in mind. In additions, many systems are designed with the ability to induce artificial leaks for periodic exercise for leak performance purposes.

The leak detection methods are often subjective. Some conventional methods and systems for pipeline leak detection had been developed, such as methods based on mass/volume balance, static decision method, transient model method and acoustic method, etc. Among these methods is acoustic method which has been proven to be the most effective, true real-time and on-line leak detection method, which provides quick leak detection, high sensitivity, accurate leak location, and low false alarm rate [2]. However, all leak detection methods are laid on understanding the fluid process properties such as pressure, mass and volumetric flow rates and temperature [3, 4].

Many leak detection and localisation methods have been used and some are currently being researched to ensure the reliability of pipelines [5-11]. These methods could generally be divided into three, namely the biological, hardware and the software methods [12]. The biological methods

* Corresponding author: Mohamed Shehadeh
Email: ezzfahmy@yahoo.com Telephone: +203-562-2366
© 2013 All rights reserved. ISSR Journals

employs trained personnel and animals like smell-sensitive dogs to locate leaking points along a pipeline, apart from the high risks involved with this method. The hardware methods as infrared thermography was used to detect hot water leaks when there is temperature increase in the surrounding environment after a leak [13]. Acoustic devices based their detection and localisation on the fact that when a leak occurs, noise is generated due to turbulence, their sensors listens to the varying noise signals and triggers an alarm. [11, 14, 15].

In last two decades, Computational Fluid Dynamics (CFD) plays a key role in the investigation of the effects of different properties of different products transported through pipelines by varying distances and operating conditions [4]. Nowadays, numerous research works were reported using general-purpose CFD solvers to study the pipeline leakages in different industrial applications [4-8]. For example, Silva et. al. [5] studied the leak detection using a computational method for analysis of hydraulic transients in pipelines. They used pressure transducers along the pipe length in order to detect and locate leaks. Also, Dobrowolski et. al. [6] used a CFD code to simulate fluid flow through a pipeline with an orifice. The influence of the turbulence model and the size of the numerical grid on the quality of the obtained results were tested. They found that the standard Launder-Spalding $k-\epsilon$ model yields the best results for two-dimensional flows through pipeline-orifice systems. Hong-Xi et. al. [7] proposed a CFD-based gas leakage and dispersion numerical simulation model. The gas distribution on the ground and variation of tracer gas concentration of monitoring points with time were estimated. The effects of terrain, wind direction and wind speed on gas dispersion were obtained. The results show a contrast between simulation and experimental results which illustrates the validity of numerical model in handling gas leakage and dispersion in complex mountainous terrain.

To that end, contemporary technology is not yet mature enough to locate the leakage as well as the leakage detection algorithms are not yet in the public domain. This paper is developing a numerical method in order to investigate the hydro-dynamics of water leakage in a horizontal pipe having relatively small cracks for addressing the effects of specific variables on the amount of leakage and the time required to achieve specific leak volumes.

2. Experimental Test Rig Description

Five series of leakage experiment has been carried out using five steel pipe segments with holes diameter of 1, 2, 3, 4 and 5 mm. Each tested pipe segment has a particular hole size and its mounted in the whole water system using two union fittings, as shown in Figure (2). The tested pipe segment was then subjected to a series of tests for various pump delivery pressures varying from 0.5 to 3 bar, see Table (1).

The general schematic diagram of the experimental test rig used in this study was designed to circulate a water flow within a closed loop system. The test rig has a total length of 8 m and a width of 2 m. A line diagram and a general view for the designed test rig are displayed in Figure (1). The whole experimental test rig was designed to allow water for circulation at flow rates up to 41 m³/hr.

The whole test rig was manufactured from carbon-steel and consists mainly of five main sections (i.e. water tank, main chassis, suction piping system, delivery piping system and pipe segment test), see Figure (1). The dimensions of the tested steel pipe segment are 1200 mm length, 53 mm diameter and 7 mm thickness. The segment pipe is connected to the test rig through two union fittings at its two ends, as shown in Figure (2). Moreover, two ball valves are used before and after the test pipe segment in order to control the water flow to facilitate the test section isolation for necessary connection or disconnection. The test rig is equipped with various different analogue pressure gauges relative to the pump speed. Table (1) presents the measured pressure at pump delivery (P_d), upstream (P_{up}), and downstream (P_{down}).

Table (1): Values of system pressures

| Reynolds Number $\times 10^5$ | P_d (bar) | P_{up} (bar) | P_{down} (bar) |
|-------------------------------|-------------|----------------|------------------|
| 1.45 | 0.5 | 0.41 | 0.35 |
| 1.79 | 1 | 0.51 | 0.49 |
| 2.18 | 1.5 | 0.69 | 0.61 |
| 2.48 | 2 | 0.85 | 0.75 |
| 2.79 | 2.5 | 1.01 | 0.90 |
| 2.95 | 3 | 1.15 | 1.01 |

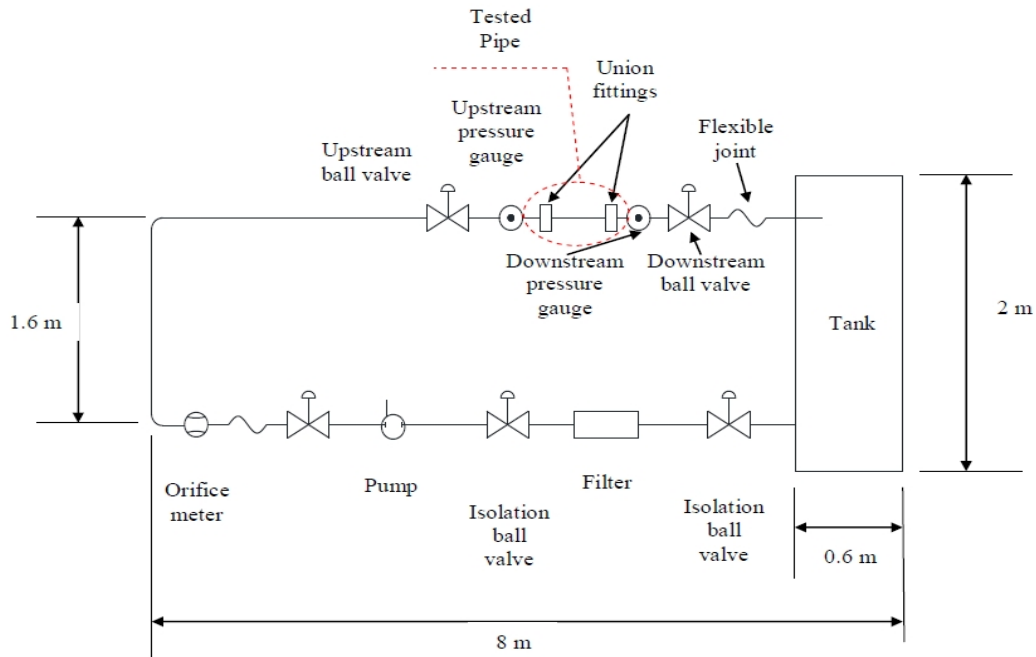


Figure (1): Schematic diagram of the experimental water system

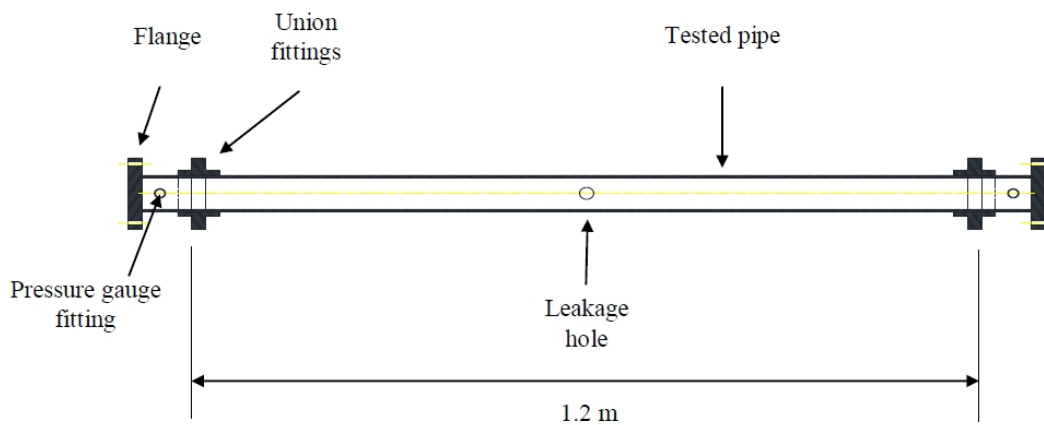


Figure (2): Tested pipe segment

3. Numerical Approach

3.1. Governing Equations

In order to assess the change in pressure, the velocity and turbulence need to be determined. These can be found by solving the governing conservation equations for mass

and momentum. Steady-state incompressible flow of water is considered. The 3D Cartesian continuity equation is given by

$$\frac{\partial u}{\partial x} + \frac{\partial v}{\partial y} + \frac{\partial w}{\partial z} = 0 \quad (1)$$

where u, v and w are the components in x, y and z directions, respectively.

The equation for the conservation of linear momentum is given by:

$$\frac{\partial(\rho u_i)}{\partial t} + \frac{\partial(\rho u_i u_j)}{\partial x_j} = \frac{\partial \tau_{ij}}{\partial x_j} \quad (2)$$

where

$$\tau_{ij} = - \left[P + \frac{2}{3} \mu \operatorname{div} u \delta_{ij} + 2\mu D_{ij} \right] \quad (3)$$

and,

$$\operatorname{div} u = \frac{\partial u}{\partial x} + \frac{\partial v}{\partial y} + \frac{\partial w}{\partial z} \quad \& \quad D_{ij} = \frac{1}{2} \left(\frac{\partial u_i}{\partial x_j} + \frac{\partial u_j}{\partial x_i} \right) \quad (5)$$

3.2. Model Assumptions

The flow model provides a baseline for the simulation of the turbulent flow, passing through the simulated leakage hole. The following assumptions are to be applied,

- The flow is isothermal.
- The flow is incompressible.
- The flow is Newtonian (i.e. the viscous stresses are proportional to the rates of deformation).
- Body Forces are neglected
- No slip condition at the wall boundaries

This model consists of two transport equations for turbulent kinetic energy (k) and dissipation rate (ε) as described in Equations (5) and (6), respectively.

$$\frac{\partial}{\partial x_j} (\rho k u_j) = \frac{\partial}{\partial x_j} \left[\left(\mu + \frac{\mu_t}{\delta_k} \right) \frac{\partial k}{\partial x_j} \right] + \mu_t \left[\frac{\partial u_i}{\partial x_j} + \frac{\partial u_j}{\partial x_i} \right] \frac{\partial u_i}{\partial x_j} - \rho \varepsilon \quad (5)$$

$$\frac{\partial}{\partial x_j} (\rho \varepsilon k u_j) = \frac{\partial}{\partial x_j} \left[\left(\mu + \frac{\mu_t}{\delta_k} \right) \frac{\partial \varepsilon}{\partial x_j} \right] + C_{s1} \mu_t \left[\frac{\partial u_i}{\partial x_j} + \frac{\partial u_j}{\partial x_i} \right] \frac{\partial u_i}{\partial x_j} \frac{\varepsilon}{k} - \rho C_{s2} \frac{\varepsilon^2}{k} \quad (6)$$

where

$$\mu_t = \rho C_\mu \frac{k^2}{\varepsilon} \quad (7)$$

The empirical constants for the turbulence model are assigned the following values in accordance respectively.

$$C_{\mu}=0.09, C_{s1}=1.47, C_{s2}=1.92, \delta_k=1, \delta_s=1.3$$

The aforementioned constants were obtained from benchmark experiments of simple flows using air and water.

3.3. Computational Domain

The layout of the pipeline model is constructed to simulate the experimental leakage pattern at rupture area. The model is designed for steel pipe schedule (40) with dimensions of 53 mm inner diameter, 60 mm outer diameter and 500 mm length, as shown in Figures (3) and (4). The leakage hole has been designed at the middle of the pipe with different diameters of 1, 2, 3, 4, and 5 mm. The input parameters of the boundary conditions used for the solution are listed in Table (1).

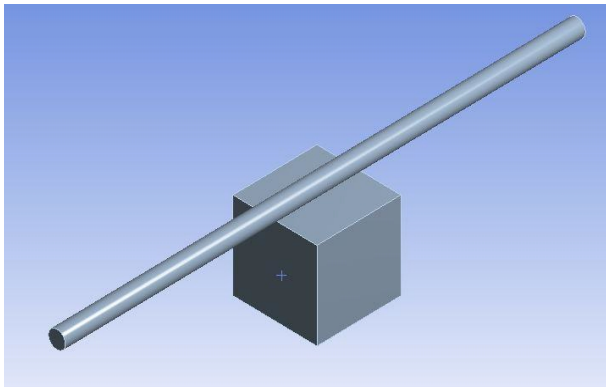


Figure (3): Modelled Pipe line

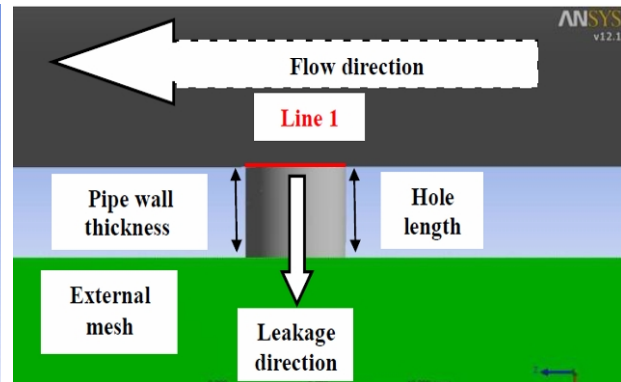


Figure (4): Modelled hole for leakage

The experimental data presented in Table (1) has been used as boundary conditions to develop the CFD model. The turbulence intensity was set to be 10 %. The wall boundary condition is defined to be a stationary wall. Moreover, the shear condition at the wall was chosen as no slip condition (i.e. $u=v=w=0$).

3.4. Mesh Generation

The coupled system of equations are solved together with its boundary conditions using finite volume technique and a second order upwind scheme with suitable under-relaxation factors of 0.8 for momentum for all case studies. The iterative procedure for the solution is considered converged when the norm of the relative errors of the solution between iterative steps is less than a tolerance of 0.001. A grid independence study was performed and a mesh of $(140 \times 140 \times 140)$ yielded satisfactory results where optimum accurate solution convergence was achieved, as shown in Figures (5) and (6),

3.5. Model Validation

In order to validate the model, the 1 mm hole diameter test case was chosen. Figure (7) shows a comparison between CFD results and experimental measurements for the effect of changing Reynolds number on the leakage mass flow rate. A reasonable agreement was found between the experimental and numerical results. Similar trends were obtained between the experimental and computational results. An increase in Reynolds number was

accompanied by an increase in the leakage mass flow rate. A maximum error of 25% was obtained at 1.79×10^5 Reynolds number.

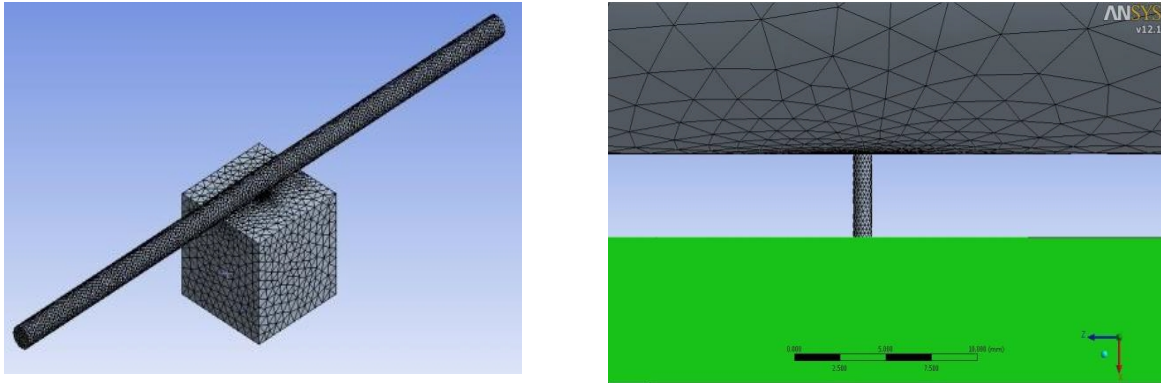


Figure (5): Meshing for the pipeline model

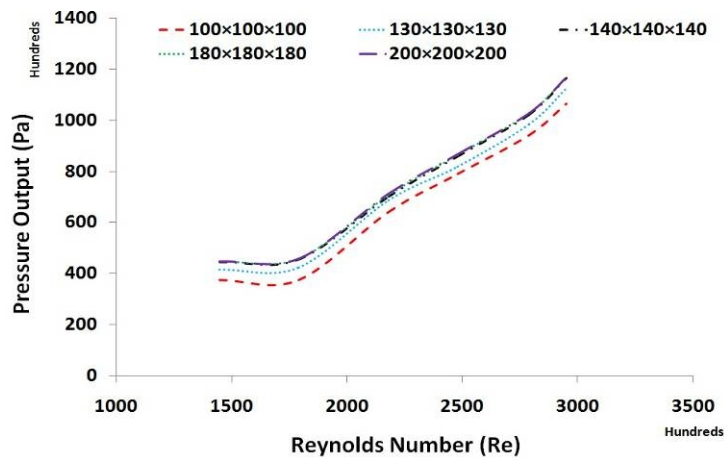


Figure (6): Grid independence study

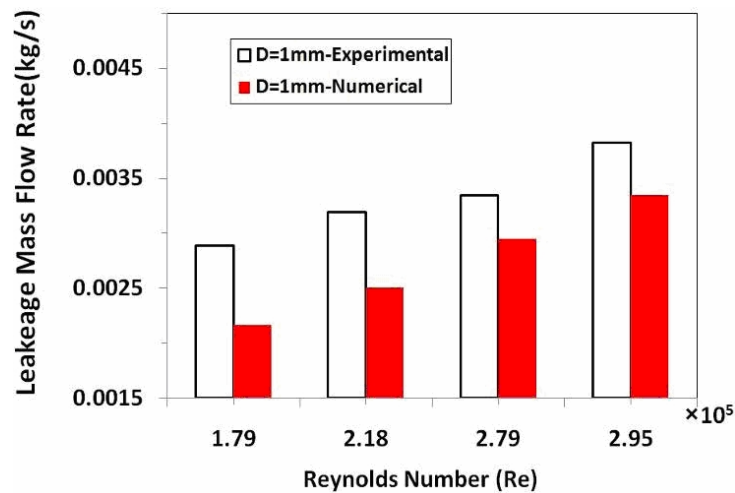


Figure (7): Validation between experimental and numerical results for hole of 1mm diameter.

4. Results

In this part, the numerical results were taken for a velocity field (velocity magnitude) and turbulence intensity to get a clear view of the leakage pattern from different simulated holes

diameter of 1, 2, 3, 4 and 5 mm along with different Reynolds numbers of 1.45×10^5 , 1.79×10^5 , 2.18×10^5 , 2.79×10^5 and 2.95×10^5 .

Figures (8) and (9) show the distribution of water velocity through for a vertical plane perpendicular to hole location for the different hole diameters and Reynolds numbers. The results showed that the hole diameter has a significant effect on the velocity magnitude. For the 5 mm hole diameter, it is clear that the velocity attained maximum value of 4.25 m/s at highest Reynolds number of 2.95×10^5 . Figures (10) and (11) show the distribution of turbulence intensity for different hole diameters and Reynolds numbers.

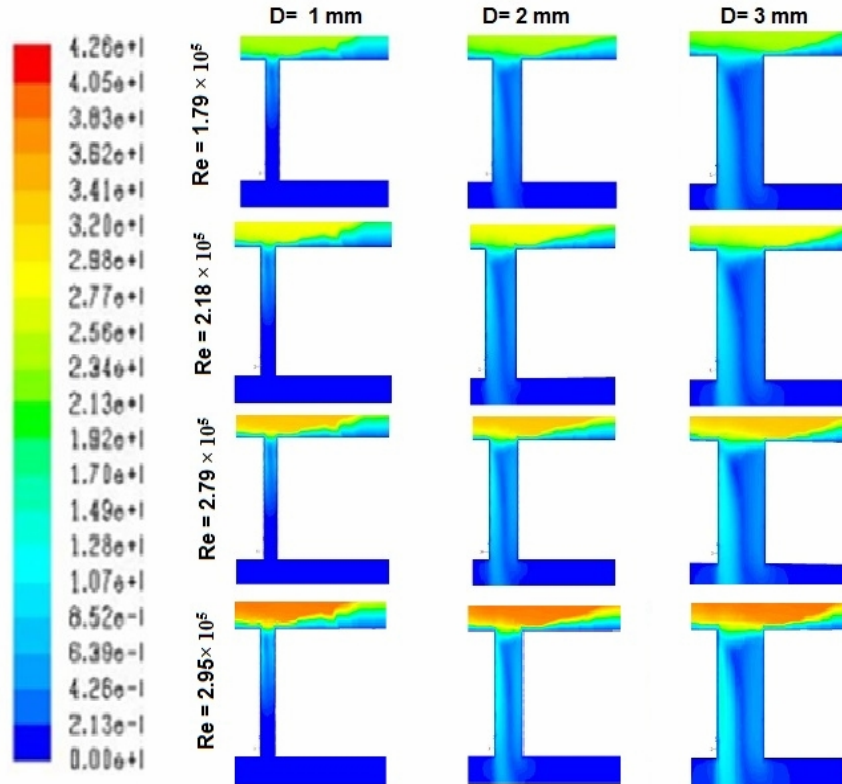


Figure (8): Velocity magnitude contours for holes of 1, 2 and 3 mm diameter.

5. Discussion

Figure (12) shows the effect of velocity magnitude on the leakage flow rate. It is shown that the increase of velocity causes an increase in the leakage flow rate for all hole diameters. It is also observed that the velocity has a minor effect for the 1 mm hole diameter as the leakage mass flow rate does not change with the increase of velocities. The maximum leakage mass flow rate was 0.08 kg/s for the 5 mm diameter at 4.25 m/s while the minimum leakage mass flow rate was 0.002 kg/s for the 1mm diameter at 2.76 m/s.

Figure (13) shows the effect of pressure drop (ΔP) on the leakage mass flow rate. It is shown that the increase of pressure drop across the hole causes an increase in the leakage mass flow rate for all hole diameters. It is also observed that the increase of pressure has a minor effect on the leakage mass flow rate for the hole of 1 mm diameter. The maximum leakage mass flow rate was 0.08 kg/s for the 5 mm diameter at 5617 Pa while the minimum leakage mass flow rate was 0.00216 kg/s for the 1mm diameter at 2466 Pa.

Figure (14) shows the effect of turbulence intensity on the leakage mass flow rate. It is clear that the leakage mass flow rate is directly proportional to turbulence intensity. It is also observed that the increase of turbulence intensity has a minor effect on the leakage mass flow rate

for 1 mm hole diameter. The maximum leakage mass flow rate was 0.08 kg/s for the 5 mm diameter at 54.5 % turbulence intensity while the minimum leakage mass flow rate was 0.00216 kg/s for the 1 mm diameter at 31 % turbulence intensity.

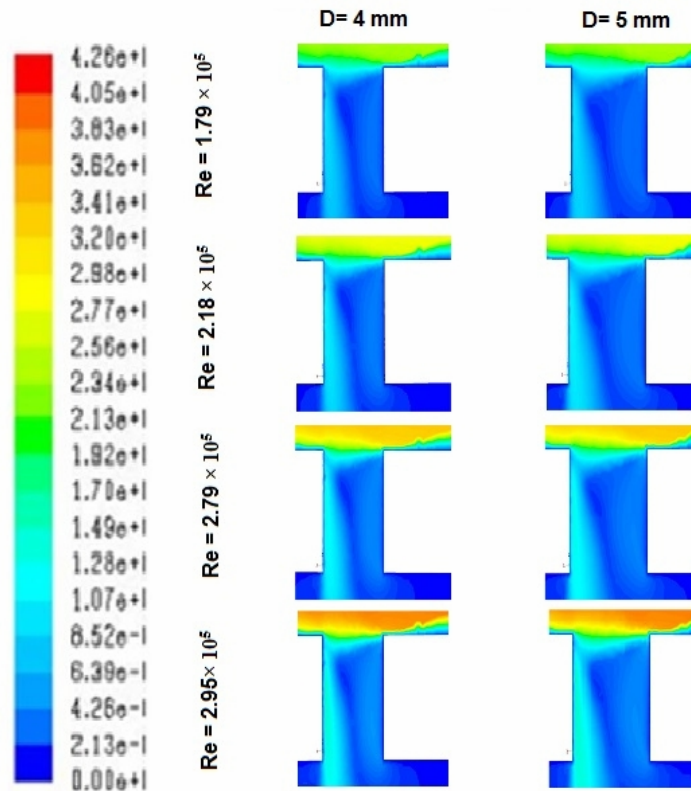


Figure (9): Velocity magnitude contours for holes of 4 and 5 mm diameter.

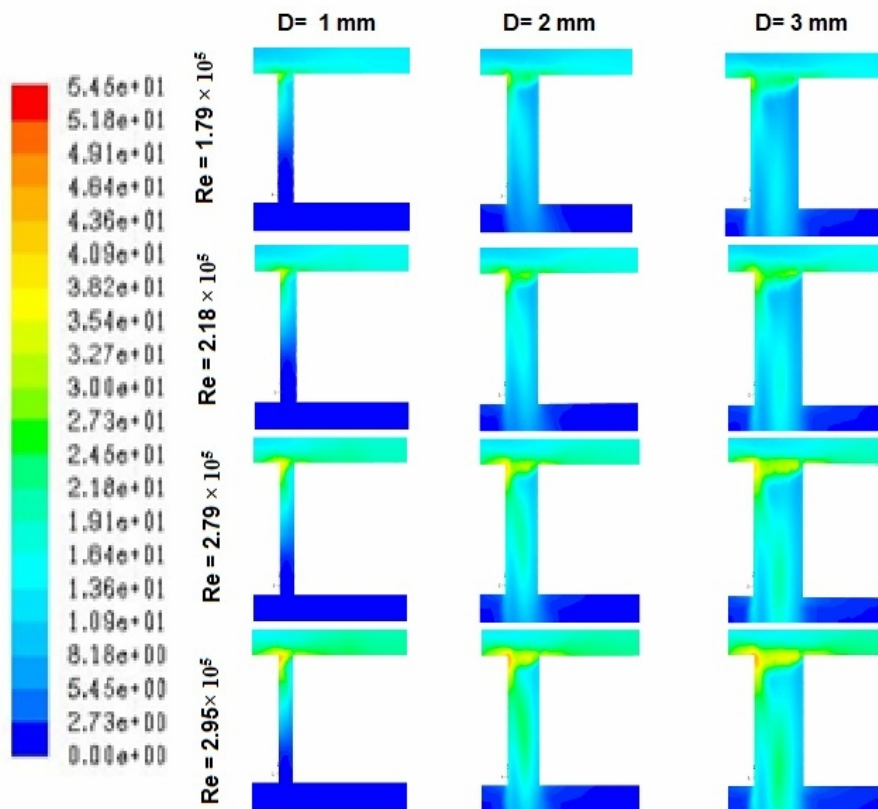


Figure (10): Turbulence intensity contours for holes of 1, 2 and 3 mm diameter.

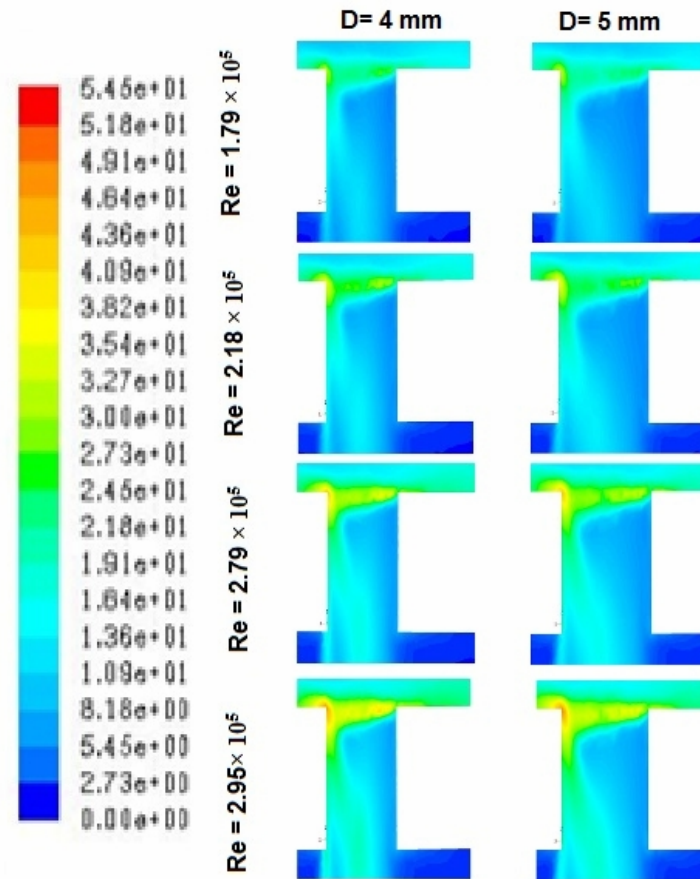


Figure (11): Turbulence intensity contours for holes of 4 and 5 mm diameter.

All flow disturbances, whether pipe fittings, valves, pumps, or leaks add to the intensity of the turbulence which present in the previous sections. Figures (12-14) present direct relations between the velocity, pressure drop and turbulence intensity with leakage mass flow rate. Accordingly, it can be clearly observed that the changes in pressure and turbulence intensity are able to detect relatively large cracks. For all hole diameters, the turbulence intensity reaches its maximum value at edge of leakage hole in the direction of flow. Accordingly, the effect of erosion-corrosion rate will be increased (e.g. [16-17]) at the edge of the leakage hole which leads to increase the rupture area.

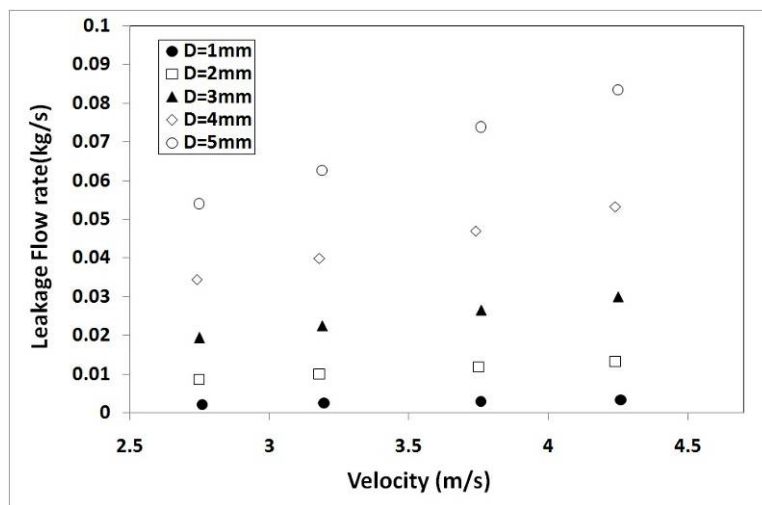


Figure (12): Velocity magnitude vs. Leakage flow rates for all holes.

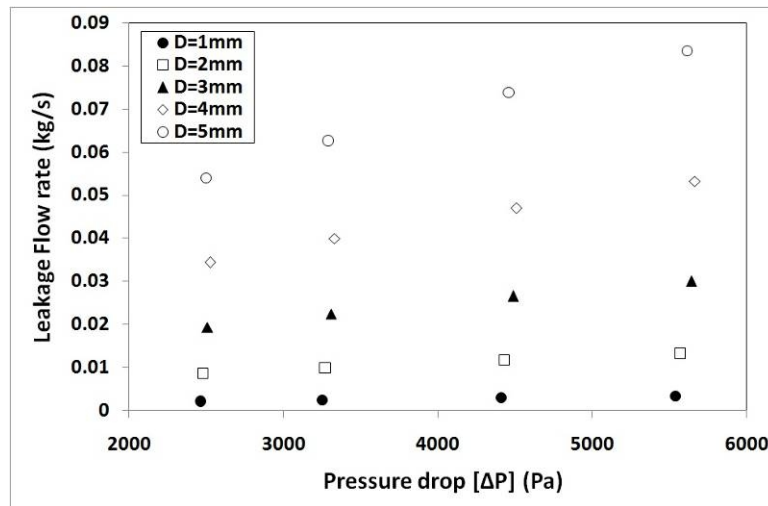


Figure (13): Pressure drop vs. Leakage flow rates for all holes.

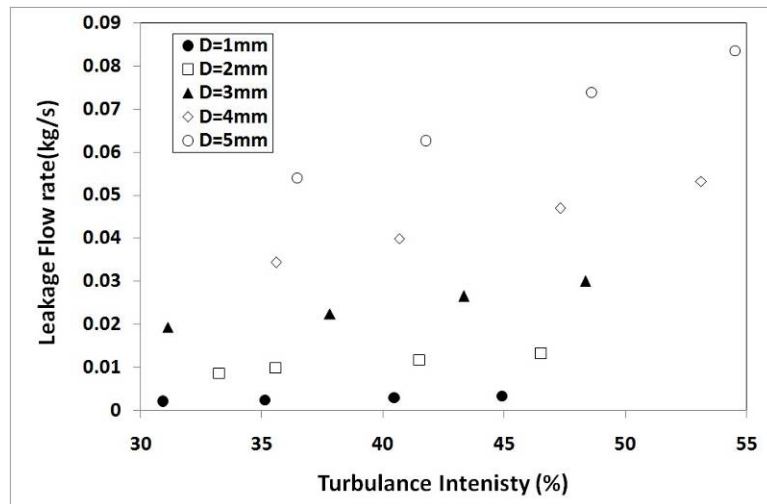


Figure (14): Turbulence intensity vs. Leakage flow rates for all holes.

6. Conclusion

A three dimensional study of flow pattern from a leakage hole in a horizontal pipeline system has been investigated using a general-purpose CFD solver. The effects of incompressible fluid flow properties as pressure, velocity, turbulence intensity and hole diameter on leakage mass flow rate have been investigated. This investigation is an attempt to bridge this gap in literature by modelling an experimental study to characterize the effect of leak hole diameter in water system via CFD Modelling. For all numerical results, it was observed that the hole diameter has a significant effect on turbulence intensity reaching of maximum 54.5 % at 5 mm diameter. Also, it was found that there was no variation in fluid properties with change of Reynolds number in the case of 1 mm hole diameter (i.e. relatively small cracks). Hence, leaks in high Reynolds number flow may be detected easier than leaks in low Reynolds number flow pipes. Finally, future studies need to be extended to different shapes of pipe rupture areas with larger Reynolds number.

References

- [1] P. Lopes dos Santos a, T-P Azevedo-Perdicolis b, G. Jank c, J.A. Ramos d and J.L. Martins de Carvalhoe, Leakage detection and location in gas pipelines through an LPV identification approach, *Communications in Nonlinear Science and Numerical Simulation*, 16 (12), 4657–4665, 2011.
- [2] Lingya Meng, Li Yuxing, Wang Wuchang and Fu Juntao, Experimental study on leak detection and location for gas pipeline based on acoustic method, *Journal of Loss Prevention in the Process Industries*, 25 (1), 90–102, 2012.
- [3] H. V. Silva, C. K. Morooka, I. R. Guilherme, T. C. Fon- seca and J. R. P. Mendes, Leak Detection in Petroleum Pipelines Using a Fuzzy System, *Journal of Petroleum Science and Engineering*, 49 (3-4), 223-238, 2005.
- [4] M. Shehadeh, A. Sharara, M. Khamis and H. El-Gamal, A Study of Pipeline Leakage pattern Using CFD, *Canadian Journal on Mechanical Sciences & Engineering*, 3(3), 2012
- [5] E.F.R.Silva, Implementing a monitoring module for a leak detection system pipeline oil Dissertation, *Dept.Elect.Eng. UFRN*, Natal, Brazil, 2009.
- [6] B. Dobrowolski, K. Krecisz and A. Spyr., Usability of Selected Turbulence Models for Simulation Flow Through a Pipe Orifice, *TASK QUARTERLY*, 9 (4), 439–448, 2006.
- [7] Hong-xi, Zhen-lin, Jian z. and Yong-xue, Numerical simulation of leakage and dispersion of acid gas in gathering pipeline, *Journal of China University of Petroleum*, 2008.
- [8] C. Verde, Multi-Leak Detection and Isolation in Fluid Pipelines, *Control Engineering Practice*, 9 (6), 673-682, 2001.
- [9] Bose J.R., Olson M.K., Taps's leak detection seeks greater precision, *Oil and Gas Journal*, 3- 47, 1993.
- [10] Carlson B. N., Selection and use of pipeline leak detection methods for liability management into the 21st century, Pipeline Infrastructure II, *Proceedings of the International Conference*, ASCE, 1993.
- [11] Turner N. C., Hardware and software techniques for pipeline integrity and leak detection monitoring, *Proceedings of Offshore Europe 91*, Aberdeen, Scotland, 1991.
- [12] Jun Zhang, Designing a Cost Effective and Reliable Pipeline Leak Detection System, REL Instrumentation Limited, Manchester, *Pipeline Reliability Conference*, Houston, U.S.A., Nov. 19- 22 , 1996
- [13] Weil G.J., Non contact, remote sensing of buried water pipeline leaks using infrared thermograph, *Water Resources Planning and Management and Urban Water Resource*, 404- 406, 1993.
- [14] Hough J.E., Leak testing of pipelines uses pressure and acoustic velocity, *Oil and Gas Journal*, 86 (47), 35-43, 1988.
- [15] Klein W. R., Acoustic leak detection, *American Society of Mechanical Engineers*, Petroleum Division, 55, 57-61, 1993.
- [16] Mohamed Shehadeh, A.I shahata, Mohamed El-Shaib and Ahmed Osman, Numerical and Experimental Investigations of Erosion-Corrosion in Carbon-Steel Pipelines, *International Journal of Applied Engineering Research*, 8 (11), 1217-1231, 2013.
- [17] M. Shehadeh and I. Hassan, Study of Sacrificial Cathodic Protection on Marine Structures in Sea and Fresh Water in Relation to Flow Conditions, *Ships and Offshore Structures*, 8 (1), 102-110, 2013.